
Article:
Andritsou, Vasiliki, De Melo, Eduardo M., Tsouko, Erminda et al. (4 more authors) (2018) Synthesis and Characterization of Bacterial Cellulose from Citrus-Based Sustainable Resources. ACS Omega. pp. 10365-10373.

https://doi.org/10.1021/acsomega.8b01315

ACS OMEGA

Article

Cite This: ACS Omega 2018, 3, 10365−10373

http://pubs.acs.org/journal/acsodf

Synthesis and Characterization of Bacterial Cellulose from Citrus-Based Sustainable Resources

Vasiliki Andritsou,[†] Eduardo M. de Melo,[‡] Erminda Tsouko,[†] Dimitrios Ladakis,[†] Sofia Maragkoudaki,[†] Apostolis A. Koutinas,*[,†] and Avtar S. Matharu*[,‡]

[†]Department of Food Science and Human Nutrition, Agricultural University of Athens, Iera Odos 75, 118 55 Athens, Greece

[‡]Green Chemistry Centre of Excellence, Department of Chemistry, University of York, Heslington, Y010 5DD York, U.K.

ABSTRACT: Citrus juices from whole oranges and grapefruits (discarded from open market) and aqueous extracts from citrus processing waste (mainly peels) were used for bacterial cellulose production by *Komagataeibacter sucrofermentans* DSM 15973. Grapefruit and orange juices yielded higher bacterial cellulose concentration (6.7 and 6.1 g/L, respectively) than lemon, grapefruit, and orange peels aqueous extracts (5.2, 5.0, and 2.9 g/L, respectively). Compared to the cellulosic fraction isolated from depectinated orange peel, bacterial cellulose produced from orange peel aqueous extract presented improved water-holding capacity (26.5 g water/g, 3-fold higher), degree of polymerization (up to 6-fold higher), and crystallinity index (35−86% depending on the method used). The presence of absorption bands at 3240 and 3270 cm^{-1} in the IR spectrum of bacterial cellulose indicated that the bacterial strain *K. sucrofermentans* synthesizes both I_α and I_β cellulose types, whereas the signals in the ^{13}C NMR spectrum demonstrated that I_α cellulose is the dominant type.

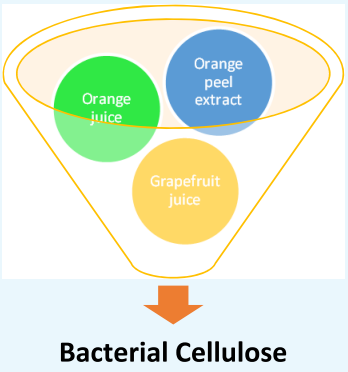

INTRODUCTION

Escalating negative environmental and societal concerns associated with utilizing traditional petrochemical processes for chemical, polymer, and material production have paved the way toward a bioeconomy era using renewable resources instead. Citrus wastes and residues represent an interesting renewable feedstock because of its wide availability and propensity to yield chemicals and materials. In 2016/2017, the worldwide citrus production, including oranges, grapefruits, and lemons, was 63.3 million tonnes, with oranges dominating market share at 80%.[1] Citrus peels constitute almost one half of the total fruit mass and are generated as low-value byproduct streams from the corresponding processing industries. Furthermore, fruits are discarded by open markets, but information on the quantities generated is scarce. Adding value to citrus processing residues and, especially, whole fruits discarded from open markets requires the development of novel biorefinery models. For instance, orange peels are being used in the development of integrated biorefineries for the production of D-limonene, pectin, and mesoporous cellulose[2,3] or fermentation products (due to its high carbohydrate content, potentially more than 80% of peel weight)[4] such as bacterial cellulose (BC),[5] biosurfactants,[6] citric acid,[7] and bioethanol.[8]

The utilization of agroindustrial waste and byproduct streams as feedstock is necessary to achieve sustainable production of bacterial cellulose. For instance, crude glycerol from biodiesel production processes and flour-rich confectionery industry waste streams have been used to produce bacterial cellulose (ca. 13 g/L) under static cultures.[9] Kuo et al.[10] used orange peel waste as substrate for bacterial cellulose production and showed outstanding performance, where yields were up to 6 times higher than conventional medium (Hestrin and Schramm).[11] The wide availability, low price, renewability, and high carbohydrate content of citrus waste makes it a good candidate as a bacterial cellulose production medium.

Bacterial (nano)cellulose is produced extracellularly at high efficiency and purity by *Acetobacter* species.[12] Bacterial cellulose is classified as a material of nanoscale network, as it is secreted in the form of ribbon-shaped fibrils of less than 100 nm comprising 2−4 nm nanofibrils.[13] Nanocellulose fibers can be applied in various industrial sectors including food industry, pharmaceutical, and electronics due to their exceptional properties, e.g., enhanced mechanical strength, high water holding capacity, and biodegradability.[14]

Various chemical, mechanical, microwave-assisted, and enzymatic methods or combinations of those have been proposed for the conversion of plant cellulose to nanostructured cellulose.[15] High production costs and not so environment-friendly processes continue to hamper the fast track development and acceptance of nanocellulose.[16]

However, bacterial cellulose can be produced under static or agitated cultures. Static cultures are simple and lead to the formation of cellulose membranes at the surface of the culture, but industrial implementation is hindered due to high production costs resulting from low productivities achieved. Agitated cultures could lead to cost-competitive production of bacterial cellulose,[17] but there remains a need to optimize operating conditions.

Received: June 12, 2018
Accepted: August 20, 2018
Published: August 31, 2018

DOI: 10.1021/acsomega.8b01315
ACS Omega 2018, 3, 10365−10373

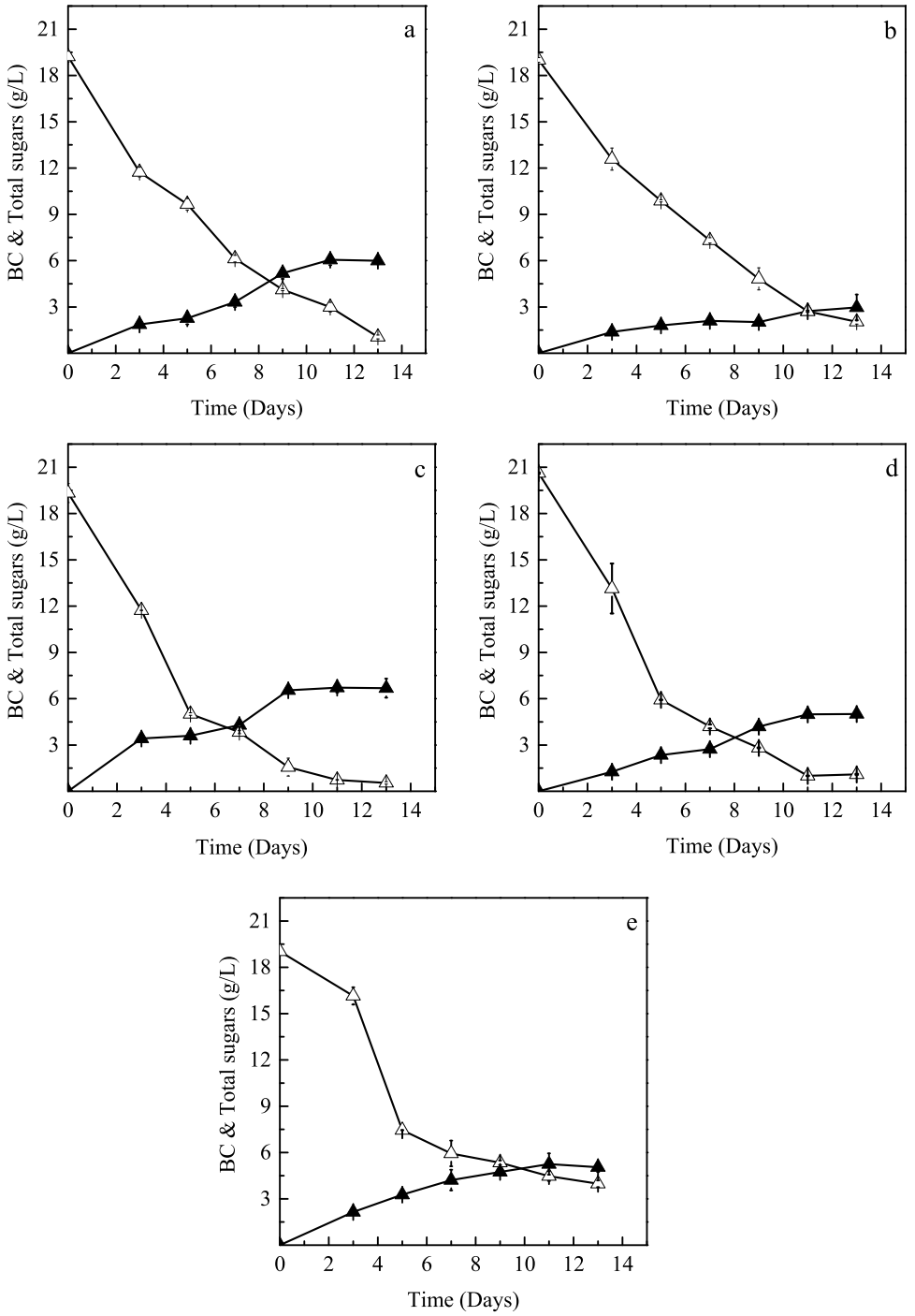

Figure 1. Consumption of total sugars (Δ) and bacterial cellulose production (▲) in shake flasks cultures of *K. sucrofermentans* using orange juice (a), orange peel extracts (b), grapefruit juice (c), grapefruit peel extracts (d), and lemon peel extracts (e).

This study evaluates the synthesis and characterization of bacterial cellulose using aqueous extracts from solid citrus processing waste or whole fruits discarded as waste from open markets. Furthermore, the key physicochemical properties of bacterial cellulose produced on orange peel aqueous extracts were identified and compared with the respective properties of cellulose isolated from orange peels.

RESULTS AND DISCUSSION

Production of Bacterial Cellulose Utilizing Citrus-Based Media. Citrus juices (orange and grapefruit) from whole fruits discarded from open markets and aqueous extracts from solid citrus waste (SCW) (orange, grapefruit, and lemon) were evaluated for their efficiency for bacterial cellulose production by the bacterial strain *Komagataeibacter sucrofermentans* DSM 15973. Figure 1 presents the total sugar consumption and bacterial cellulose production in shake flask fermentations of *K. sucrofermentans* cultivated on orange and grapefruit juices and aqueous extracts from orange, grapefruit, and lemon SCW peels. The cultivation of *K. sucrofermentans* in grapefruit juice-based media led to the highest bacterial cellulose concentration (6.7 g/L), yield (0.36 g bacterial cellulose per g

DOI: 10.1021/acsomega.8b01315
ACS Omega 2018, 3, 10365−10373

consumed sugars), and productivity (0.61 g/L/day) after 11 days. The bacterial cellulose production achieved via bacterial cultures in grapefruit peel extracts (5.0 g/L), orange juice (6.1 g/L), and lemon peel extracts (5.2 g/L) is also promising. The lowest bacterial cellulose concentration (2.9 g/L) was produced after 13 days when orange peel extracts were used. The consumed sugar to bacterial cellulose conversion yield achieved was higher than 0.17 g/g, whereas productivity was higher than 0.25 g/L/day. At 11 days for all fermentations, the initial sucrose and glucose present in the media used were assimilated at 81.7−100 and 65.7−100%, respectively, whereas the assimilation of fructose varied within the range of 68.3−90.8%. The consumption of total sugars was in the range of 76.5−96.2% at 11 days for all cultures used.

Several studies have investigated bacterial cellulose production using various agroindustrial resources leading up to 10.8 g/L of bacterial cellulose concentration.[21−26] Moon et al.[27] reported the production of 18 g/L BC concentration by the strain *Acetobacter xylinum* KJ1 cultivated on saccharified food wastes in a 30 L bioreactor. There are few reported studies on the utilization of fruit-based fermentation media for BC production. Kurosumi et al.[5] evaluated juices from oranges, pineapples, apples, Japanese pears, and grapes as fermentation feedstocks for bacterial cellulose production, with orange juice demonstrating the highest bacterial cellulose concentration (5.9 g/L) after 14 days of incubation. Castro et al.[28] reported the ability of *Gluconacetobacter swingsii* sp. to grow and produce bacterial cellulose on pineapple peel juice (2.8 g/L) and sugar cane juice. Adebayo-Tayo et al.[29] reported the utilization of pawpaw juice for the production of 7.7 g/L of BC concentration. The BC production (up to 6.7 g/L) achieved in this study are among the highest reported on fruit-based media.

Morphology of Cellulose Samples. Figure 2 shows selected scanning electron microscopy (SEM) micrographs of the different cellulose samples. Whereas bacterial cellulose (Figure 2a) is formed by long fibrous network of cellulose microfibrils (D = 50−100 nm, L = several micrometers), conventional pectin extraction (CAE)-CB (Figure 2b) and OPEC-CB (Figure 2c) give a more compacted structure, where the amorphous matrix covers/binds the cellulose microfibrils matrix. Hence, in these samples, the cellulose microfibrils are not as visible as in bacterial cellulose.

Infrared Spectroscopy. The attenuated total reflection infrared (ATR-IR) spectrum of CAE-CB, OPEC-CB, bacterial cellulose, and microcrystalline cellulose (MCC) are presented in Figure 3. Besides cellulose, the CAE-CB and OPEC-CB samples also contain residual pectin, hemicellulose (mainly evidenced by uronyl residues bands at ca. 1710−1740, 1610−1630, 1430−1455, and 1250 cm^{-1}), and small amounts of lignin, phenolics, and possibly traces of proteins (mainly due to aromatic and amide characteristic absorptions at ca. 1600−1650, 1550−1450, and 1260−1180 cm^{-1}).[30−32] Due to the absence of pectin and hemicellulose, bacterial cellulose and MCC present similar absorption bands.

The main IR absorption bands appearing in all samples are summarized in Table 1. The two bands that appear approximately at 1540 and 1640 cm^{-1} in the spectrum of bacterial cellulose correspond to amide bond and can be associated with remaining proteins from the culture medium or residual bacterial biomass that was not completely separated during washing of bacterial cellulose membranes. According to Sugiyama et al.,[33] absorption bands of cellulose samples around 750 and 3240 cm^{-1} show the existence of type I_α crystalline cellulose, whereas absorption bands around 710 and 3270 cm^{-1} show the existence of the amorphous type I_β. In the IR spectra of bacterial cellulose samples, the presence of 3240 and 3270 cm^{-1}

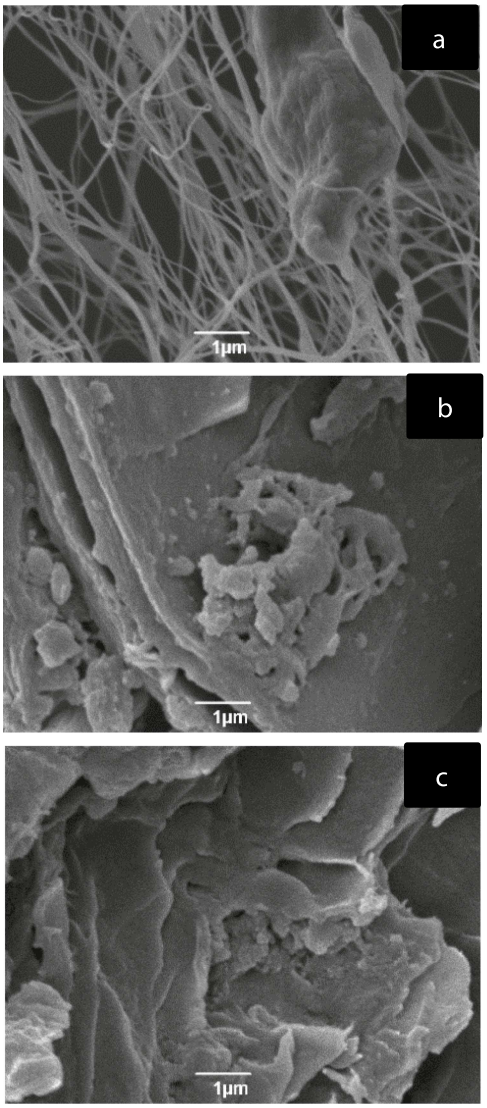

Figure 2. SEM of bacterial cellulose (a), CAE-CB (b), and OPEC-CB (c) samples.

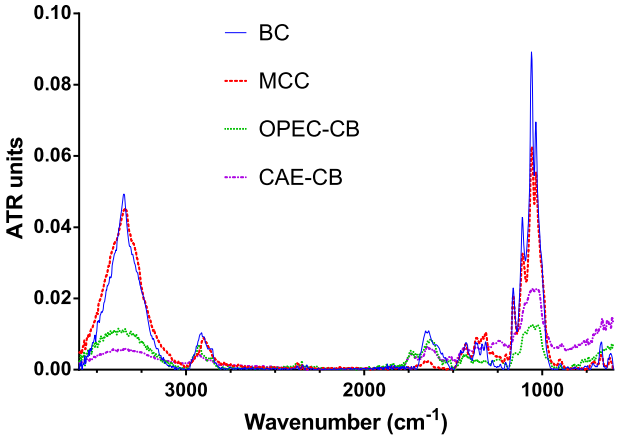

Figure 3. Infrared spectra of MCC (red), bacterial cellulose (blue), CAE-CB (purple), and OPEC-CB (green).

DOI: 10.1021/acsomega.8b01315
ACS Omega 2018, 3, 10365−10373

Table 1. Absorption Bands Present in the Spectra of Microcrystalline Cellulose (MCC), Bacterial Cellulose (BC), and Orange Peel Residues after Conventional Pectin Extraction (CAE-CB) and OPEC Process (OPEC-CB)

adsorption band (cm^{-1})	assignment
3600−3000	O−H group stretching
2895	C−H stretching in cellulose skeleton
1740−1700	−C═O stretch
1645−1630	absorbed water
1493−1396	H−C−H, O−C−H in-plane bending
1315	CH_2 rocking vibration at C6 carbon
1296−1219	out of plane bending vibration of C−O−H at C6
1205	symmetrical stretching vibration from C−O−C
1162	asymmetric stretching vibrations from C−O−C
1140−926	C−C, C−OH, C−H ring and side group vibrations
1107	C−O−C (1−4) glycosidic linkages
898	C−O−C, CC−O, C−C−H deformation and stretching vibrations

bands that are characteristic of cellulose I_α and I_β, respectively, shows that bacterial cultures produce both polymorphs during fermentation.

Thermogravimetric Analysis (TGA). According to the TGA data shown as derivative thermogravimetric traces in Figure 4 and Table 2, all samples presented a maximum

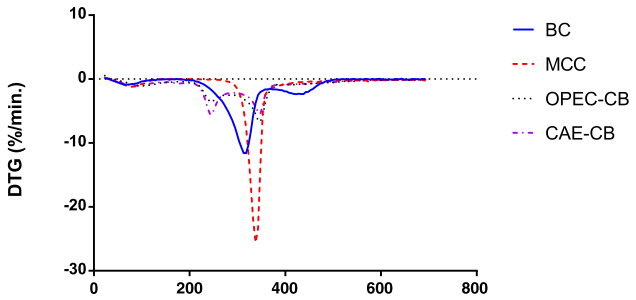

Figure 4. Derivative thermogravimetric traces of MCC (red), CAE-CB (purple), OPEC-CB (black), and bacterial cellulose, BC (blue).

Table 2. Decomposition Temperature of Microcrystalline Cellulose (MCC), Bacterial Cellulose, and Orange Peel Residues after Conventional Pectin Extraction (CAE-CB) and OPEC Process (OPEC-CB)

sample	decomposition temperature (°C)	relative pectin content (%)
MCC	339.2 ± 0.7	N/A
CAE-CB	346.6 ± 0.2	20
OPEC-CB	346.8 ± 0.5	14
bacterial cellulose	315.8 ± 0.3	N/A

degradation temperature around 315−340 °C corresponding to the decomposition of cellulose, which shows considerable thermostability.[30,31] Moreover, the derivative thermogravimetric (dTG) traces of CAE-CB and OPEC-CB show three decomposition intervals, corresponding to the elimination of water under 180 °C, breakdown of pectin and hemicellulose at the range of 220−260 °C and decomposition of cellulose at 310−380 °C.[30,31] The differences in the decomposition trace of CAE-CB and OPEC-CB samples lie on the fact that the CAE-CB contains, relatively, more pectin than OPEC-CB (Table 2). As expected, MCC and bacterial cellulose, as pure cellulose materials, do not present decomposition bands characteristic of pectin and hemicellulose.

Powder X-ray Diffraction (XRD) Analysis. Figure 5 shows the XRD diffractograms of MCC, CAE-CB, OPEC-CB, and bacterial cellulose. The diffraction peaks at 2θ = 14.5, 16.6, and 22.6° correspond to cellulose structure. These peaks are attributed to the (1 0 0), (0 1 0), and (1 1 0) planes of cellulose I_α or the (1 1 0), (1 1 0), and (2 0 0) planes of cellulose I_β.[32] It is not trivial to distinguish the two allomorphs based exclusively on the XRD peak positions due to their small distance.[34] Bacterial cellulose and MCC present more defined crystalline cellulose peaks than CAE-CB and OPEC-CB. This occurs probably due to the higher amorphous content on those latter samples, evidenced by the larger amorphous contribution band with maximum ca. 18°.

^{13}C Solid-State NMR. According to the ^{13}C cross-polarization magic angle spinning (CPMAS) NMR spectrum (Figure 6), the signals that correspond to the six carbons of cellulose molecule were identified in all samples. C_1 corresponds to the signal at 105 ppm, C_4 at 89.1 ppm, C_3 at 75.12 ppm, C_2 and C_5 at 72.6 ppm, and C_6 at 65.4 ppm. In the spectrum of bacterial cellulose, the enhanced downfield resonance line for C_4 triplet and the strong central resonance line for C_1 crystalline indicate that cellulose I_α is dominant.[35] CAE-CB and OPEC-CB samples presented extra signals because of the presence of other components. Signals at 174 and 53.9 ppm in CAE-CB and OPEC-CB correspond to carbonyl and methyl-ester group of pectin, respectively.[15]

Crystallinity Index. Crystallinity index depends significantly on the instrument used and the data analysis method applied. According to Park et al.,[36] the ATR-IR spectroscopy is the most convenient method (resulting in a ratio of crystalline to amorphous content), whereas XRD and NMR methods provide more accurate values of crystallinity index resulting in percentage values. Bacterial cellulose demonstrated the highest crystallinity index in all the examined methods followed by MCC, OPEC-CB, and CAE-CB (Table 3). As observed in Figure 3, the IR bands related to the crystallinity index of cellulose present in CAE-CB and OPEC-CB overlap with absorptions from other compounds bounded with cellulose, such as pectin and hemicellulose. Hence, the presence of these amorphous polysaccharides can underestimate the crystallinity index calculated from the IR data. Moreover, according to Liitiä et al.[37] and Bernardinelli et al.,[38] hemicellulose, lignin, and disordered cellulose in plant biomass resonate in the amorphous NMR spectral region and interfere with cellulose crystallinity. The XRD diffractions will also contain contributions from amorphous matter in the samples. Consequently, the determination of the crystallinity index by those techniques are restricted to result only in relative values of crystallinity index (standards would be required). However, values of crystallinity index calculated from NMR, IR, and XRD were consistent in relation to each other, and XRD, in particular, seems to have given the most realistic crystallinity index values.

OPEC-CB crystallinity index values are higher than those of CAE-CB due to the lower content of pectin ("amorphous matter") in the former (see Table 2), which reflects the higher depectination power of the microwave acid-free treatment vs conventional acid treatment.

Degree of Polymerization. Table 4 presents the degree of polymerization of MCC, CAE-CB, OPEC-CB, and bacterial cellulose. Bacterial cellulose had the highest degree of polymerization (1620), whereas MCC showed the lowest

DOI: 10.1021/acsomega.8b01315
ACS Omega 2018, 3, 10365−10373

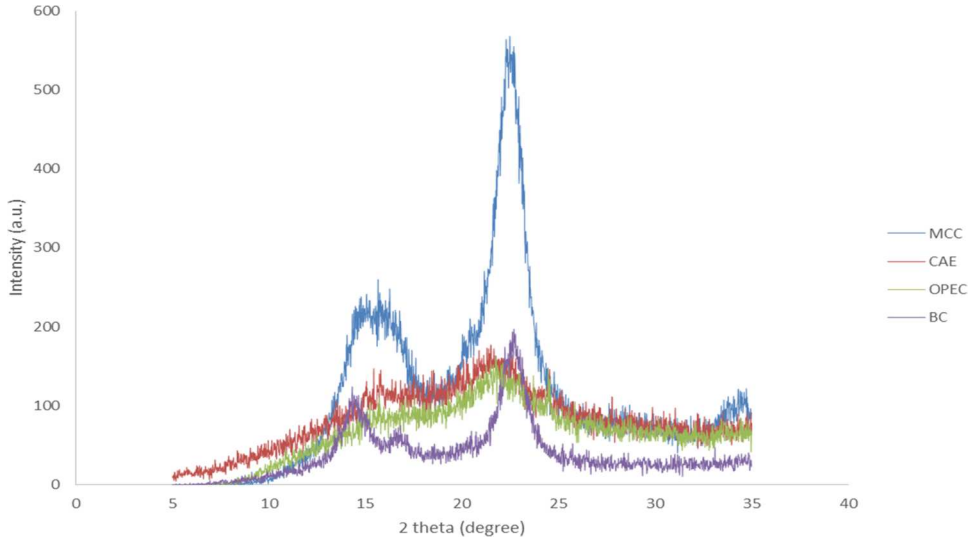

Figure 5. X-ray diffraction patterns of MCC (blue), CAE-CB (red), OPEC-CB (green), and bacterial cellulose, BC (purple).

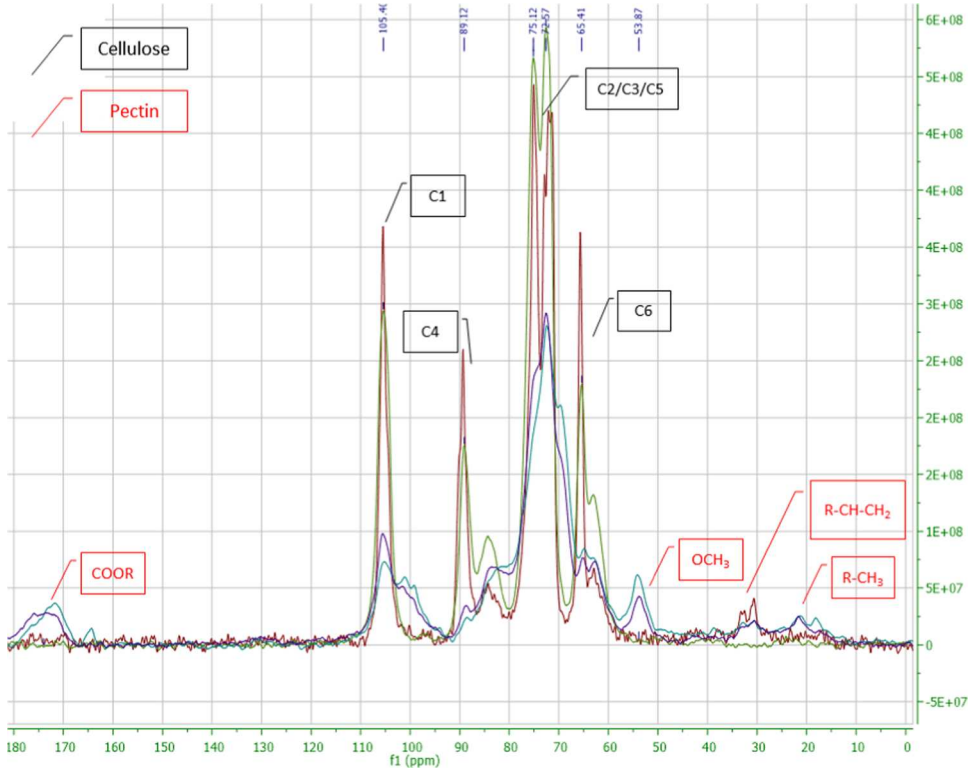

Figure 6. Solid-state ^{13}C NMR spectra of MCC (green), CAE-CB (blue), OPEC-CB (purple), and bacterial cellulose, BC (red).

Table 3. Crystallinity Index of MCC, CAE-CB, OPEC-CB, and Bacterial Cellulose Identified by XRD, IR, and ^{13}C Solid NMR

	crystallinity index		
sample	XRD (%)	IR (ratio Cr/Am)[a]	NMR (%)
MCC	84 ± 5.14	2.5 ± 0.03	50 ± 1.25
CAE-CB	53.3 ± 3.01	1.3 ± 0.01	16.1 ± 1.29
OPEC-CB	56.4 ± 4.89	1.5 ± 0.01	22.2 ± 1.06
bacterial cellulose	86.9 ± 2.23	9.7 ± 0.51	69 ± 4.02

[a]Ratio of crystalline to amorphous content.

Table 4. Degree of Polymerization of MCC, CAE-CB, OPEC-CB, and Bacterial Cellulose

sample	degree of polymerization
MCC	134 ± 26.63
CAE-CB	1250 ± 0.69
OPEC-CB	269 ± 16.35
bacterial cellulose	1620 ± 1.35

value (134). The degree of polymerization of CAE-CB seems to be almost 6-fold higher than that of OPEC-CB, which expresses the high efficiency of the microwave treatment regarding pectin extraction and biomass deconstruction. However, it is important

DOI: 10.1021/acsomega.8b01315
ACS Omega 2018, 3, 10365−10373

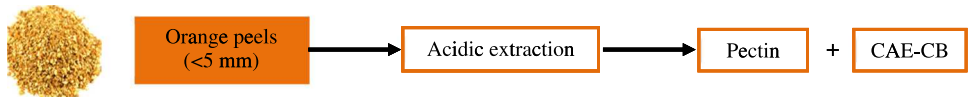

Figure 7. Conventional acidic extraction of pectin under reflux at 90 °C.

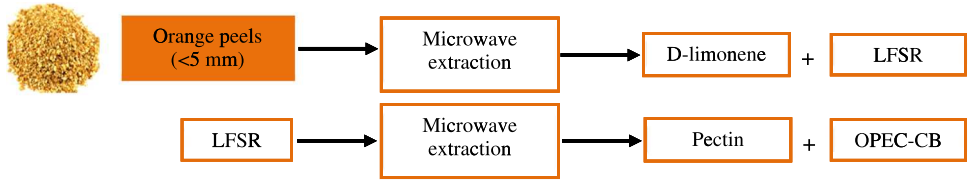

Figure 8. OPEC process for D-limonene and pectin extraction.

to consider the limitation of this analysis to those samples, once they comprise other biomolecules besides cellulose, which can interfere with the analysis accuracy.

Water-Holding Capacity (WHC). The WHC is considered one of the most important physical properties of bacterial cellulose membranes, especially for biomedical applications. The WHC of bacterial cellulose is remarkably higher (26.5 g/g) than that of CAE-CB (7.6 g/g) and OPEC-CB (7.9 g/g) samples. This is attributed to its nanofibril network (see Figure 2) that allows more water to be bound. The WHC of bacterial cellulose produced in this study is in good agreement with literature-cited publications, with similar[35] or even higher[39] values. Considering CAE-CB and OPEC-CB samples, their WHC is comparable to banana dietary fibers (6.7−10.5 g/g).[40]

CONCLUSIONS

This study showed that citrus juices derived from whole fruits discarded as waste from open markets and aqueous extracts from citrus peels produced as low-value waste streams from citrus-processing industries could be efficiently used for bacterial cellulose production. The properties of bacterial cellulose produced from citrus-based fermentations demonstrate superior properties to cellulose isolated from orange peels. However, as presented by de Melo et al.,[15] it is possible to further process those cellulosic residues by means of microwave hydrothermal treatment to yield nanocellulose, which is a material with similar properties to bacterial cellulose and presents superior hydration properties in relation to its precursors.

EXPERIMENTAL SECTION

Raw Materials. Citrus fruits (oranges and grapefruits) were obtained *ex gratia* from a local open market in Athens, Greece, as discarded (waste) fruits. Solid citrus wastes (SCW, peel, and pulp residue after juice processing) of orange, grapefruit, and lemon were obtained from local shops.

Microorganisms. The bacterial strain *K. sucrofermentans* DSM 15973 was used as cellulose producer. Preculture media were prepared as proposed by Hestrin and Schramm.[11] Bacterial cultures were stored at 4 °C in 2% (w/w) agar Petri dishes supplemented with 1% (w/w) glucose, yeast extract, and peptone.

Depectination of Orange Peel. *Conventional Acidic Extraction of Pectin.* Orange peels (<5 mm, 80 g) were added to 250 mL deionized water adjusting the pH to 1.5 with 0.5 M HCl. The mixture was heated at 90 °C for 1 h. The liquid phase containing pectin was separated from the remaining solid residue by vacuum filtration. The remaining solid residue mainly consisting of cellulosic matter (CAE-CB) was dried at 30 °C for 24 h and weighed. Figure 7 summarizes the procedure.

Acid-Free Microwave-Assisted Extraction of Pectin. Orange peels (<5 mm, 150 g) were added in a 2 L Pyrex vessel. The microwave reactor was operated at 1200 W for 6 min and subsequently at 800 W for 19 min. At the end of the process, the remaining solid residue was about 34% of the initial. The D-limonene-free solid residue (LFSR) was subsequently submitted to pectin extraction using a microwave reactor (CEM MARS 6, One Touch Technology) and closed containers (EasyPrep Plus EasyPrep Teflon) of 100 mL. In each run, six containers were filled with 4 g of LFSR sample and 70 mL of deionized water. The equipment was operated under high agitation at 120 °C for 15 min at max. power of 1800 W. The resulting mixture was vacuum filtered. The filtrate (cellulosic matter, OPEC-CB) was dried at 30 °C for 24 h and weighed. The process is summarized in Figure 8.

Formation of Nutrient-Rich Solid Citrus Waste Extracts for Bacterial Fermentations. After juice extraction, SCW were collected and mixed with water in a liquid-to-solid ratio of 3:1 and boiled for 1 h. The liquid phase was separated from the solid residues with filter paper and the sugar and free amino nitrogen (FAN) concentrations were determined (Table 5). The SCW extracts were stored at −20 °C until further use.

Table 5. Sugar and FAN Content of Citrus Juices and Aqueous Extracts from Citrus Peels

media	sucrose (g/L)	glucose (g/L)	fructose (g/L)	total (g/L)	FAN (mg/L)
Citrus Juices					
orange	19.2	39	35.5	93.4	292.4
grapefruit	15.7	37.9	34.6	88.2	275.3
Aqueous Extracts from Citrus Peels					
orange	2.7	8	7.2	17.9	69.6
grapefruit	1.4	7.2	7.1	15.7	53.6
lemon	0.2	2.3	2.1	4.6	49.4

Bacterial Cellulose Production. Bacterial fermentations with *K. sucrofermentans* were conducted in 250 mL Erlenmeyer flasks and 50 mL working volume at 30 °C. All the flasks were inoculated with 10% (v/v) preculture media and the pH value of the broth was adjusted to 6 using 5 M aqueous NaOH. The flasks were initially incubated at 150 rpm for 1−2 days and then statically. The total duration of the experiments was 13 days. Before fermentation, the nutrient composition of aqueous extracts from SCW and juices derived from whole citrus fruits discarded from open markets were properly adjusted according

DOI: 10.1021/acsomega.8b01315
ACS Omega 2018, 3, 10365−10373

to Hestrin and Schramm fermentation media.[11] All media were filter-sterilized using a 0.22 μm filter unit (Polycap AS, Whatman Ltd., Buckinghamshire, U.K.). The initial FAN and total sugar concentration in all cases were 249 ± 25 mg/L and 19.5 ± 0.7 g/L, respectively. All citrus juices were applied as the sole carbon sources for bacterial cellulose production. However, in the case of SCW aqueous extracts, their initial total sugar concentration was lower than that of citrus juices. Thus, to reach the desirable total sugar concentration, the SCW aqueous extracts were supplemented with commercial sugars using the same sugar ratio of each individual extract. Sugar supplementation was carried out in this study to evaluate the potential for bacterial cellulose production. Process development should resort to concentration of SCW aqueous extracts via reverse osmosis. Five sets of experiments were carried out using citrus juices (orange, grapefruit) and SCW extracts (orange, lemon, and grapefruit) as fermentative media. *K. sucrofermentans* could not grow on lemon juice media probably due to its high acidity and the high amount of NaOH required for adjusting the initial pH of this medium to 6. Sampling was carried out in predetermined intervals to monitor sugar and FAN consumption along with bacterial cellulose production.

Characterization of CAE-CB, OPEC-CB, and Bacterial Cellulose. The properties of isolated CAE-CB and OPEC-CB, obtained from depectination of orange peels, and bacterial celluloses, produced from orange citrus waste extracts, were analyzed with respect to purity (infrared spectroscopy), decomposition temperature (thermogravimetric analysis), crystallinity index (infrared spectroscopy, X-ray diffractometry, NMR), degree of crystallinity (^{13}C solid-state NMR), degree of polymerization, and water-holding capacity (WHC). Sample morphology characterization was performed via scanning electron microscopy (SEM).

Infrared Spectroscopy. Attenuated total reflectance infrared spectroscopy (ATR-IR) measurements were performed on a Bruker Vertex 70 instrument. Commercial microcrystalline cellulose (MCC) was used as the reference material. Spectra were recorded from 3600 to 600 cm^{-1} at 16 scans, 32 scans background scan time with a spectral resolution of 4 cm^{-1}.

Thermogravimetric Analysis. Thermogravimetric analysis (TGA) was performed using NETZSCH STA 409. Fifty milligram of sample was precisely weighed into a TGA cup and heated under nitrogen flow of 50 mL/min to avoid sample oxidation. The temperature increased from room temperature up to 700 °C at 10 K/min rate.

^{13}C Solid-State NMR. ^{13}C{1H} CPMAS spectra were acquired using a 400 MHz Bruker Avance III HD spectrometer equipped with a Bruker 4 mm H(F)/X/Y triple-resonance probe and 9.4T Ascend superconducting magnet. The CP experiments employed a 1 ms linearly ramped contact pulse, spinning rates of 12 000 ± 2 Hz, recycle delays of 5 s, spinal-64 heteronuclear decoupling (at ν_{rf} = 85 kHz), and a sum of 512 co-added transients. Chemical shifts are reported with respect to tetramethylsilane and referenced using adamantane (29.5 ppm) as an external secondary reference.

X-ray Diffractometry. X-ray diffractometry (XRD) patterns of the samples were recorded using a Bruker D8 powder diffractometer equipped with a Cu source and PSD Lynxeye detector. The samples were ground to a powder before analysis or lyophilized when referring to bacterial cellulose. The samples were scanned over a 2θ range between 5 and 90° and a θ range between 2.5 and 45° for 8.38 min, with each step recorded at 0.1 s interval. Generator voltage and filament emission were set to 40 kV and 40 mA, respectively. Data were processed using an EVA software.

Degree of Polymerization. Lyophilized samples (0.25 g) were dissolved in 50 mL copper(II) ethylenediamine solution (0.5 M). The relative viscosity (η_r) and specific viscosity (η_{sp}) of each sample in copper−ethylenediamine solution were measured using a Cannon-Fenske Routine Viscometer immersed in a water bath at constant temperature (25 ± 0.5 °C) and then calculated according to eqs 1−3

$$\eta_r = \frac{t}{t_0} \tag{1}$$

$$\eta_{sp} = \eta_r - 1 \tag{2}$$

$$\eta = \sqrt{2(\eta_{sp} - \ln \eta_r)/c} \tag{3}$$

where t_0 is the flow time of the solvent, t is the flow time of the solution, η is the intrinsic viscosity, and c is 0.5 g/dL.

The average molecular weight (M) was determined by the Mark−Houwink empirical equation (eq 4)

$$\eta = K \times M^{\alpha} \tag{4}$$

where α is equal to 0.905 and K is equal to 1.33 × 10^{-4} dL/g.

For the particular polymer−solvent system, the Mark−Houwink parameters, α and K.[18] The degree of polymerization (eq 5) was calculated as M of the polymer divided by the molecular weight of an anhydroglucose monomeric unit:

$$\mathrm{DP} = \frac{M}{162} \tag{5}$$

Crystallinity Index. This study implemented three different methods for crystallinity index determination, namely, infrared spectroscopy, ^{13}C solid-state NMR, and XRD. The method used in the present study was the peak-height method described by Segal et al.[19] The IR crystallinity index of cellulose was evaluated as the intensity ratio between IR absorption bands at 1427 and 895 cm^{-1}, which are assigned to CH_2 bending mode and deformation of anomeric CH, respectively. The calculation of the XRD crystallinity index of cellulose was calculated using the peak intensity method (eq 6)

$$\mathrm{CrI} = \frac{I_{002} - I_{AM}}{I_{002}} \times 100 \tag{6}$$

where CrI is the crystallinity index, I_{002} is the maximum intensity of the lattice diffraction, and I_{AM} is the intensity diffraction at 2θ (~23°).

Solid-state ^{13}C NMR crystallinity index was determined by separating the C_4 region of cellulose spectrum into crystalline and amorphous peaks and calculated by dividing the area of the crystalline peak (87−93 ppm) by the total area assigned to the C_4 peak (80−93 ppm) (%).

Water-Holding Capacity. Dry sample of 0.25 g was mixed with 25 mL of distilled water and left for 1 h at room temperature. After centrifugation at 3000 rpm for 20 min, the pellet was weighed and the WHC was calculated as g of water absorbed per g of dry sample.

Scanning Electron Microscopy. The surface and morphology of the samples were evaluated by SEM (Jeol JSM-6360). The lyophilized samples were coated with gold and examined at an accelerated voltage of 20 kV and magnification of 20 000×.

High-Performance Liquid Chromatography. The concentration of sugars was determined by high-performance liquid

DOI: 10.1021/acsomega.8b01315
ACS Omega 2018, 3, 10365−10373

chromatography (Prominence, Shimadzu, Kyoto, Japan) equipped with an Aminex HPX-87H (BioRad, Hercules, CA) column, coupled to a differential refractometer (RID-10A, Shimadzu, Kyoto, Japan). The mobile phase was a 10 mM H_2SO_4 aqueous solution with 0.6 mL/min flow rate. FAN concentration was assayed by the ninhydrin colorimetric method.[20]

Wet bacterial cellulose membranes were removed from the fermentation broth and rinsed with water. The resultant membranes were immersed in 1 M aqueous NaOH, boiled for 30 min, and finally washed repeatedly until a neutral pH was obtained. The dry weight of bacterial cellulose was determined either by drying the produced bacterial cellulose at 35 °C for 48 h and subsequently cooled in a desiccator or by lyophilizing the samples.

All analyses were performed in triplicate and the presented values correspond to average values.

AUTHOR INFORMATION

Corresponding Authors

*E-mail: akoutinas@aua.gr (A.A.K.).
*E-mail: avtar.matharu@york.ac.uk (A.S.M.).

ORCID

Avtar S. Matharu: 0000-0002-9488-565X

Funding

The authors from the University of York would like to thank CNPq—Conselho Nacional de Desenvolvimento Científico e Tecnológico (Brazil)—for scholarly funding Eduardo Melo to undertake research at University of York, U.K. (234010/2014-2). A.S.M. would like to acknowledge the EPRSC for funding Systems Change: Whole systems understanding of unavoidable food supply chain waste for re-nutrition (EP/P008771/1) enabling circular economy and food waste discussions with fellow co-authors from Agricultural University of Athens. The authors from the Agricultural University of Athens would like to acknowledge the financial support provided by the research project entitled INVALOR: Research Infrastructure for Waste Valorization and Sustainable Management implemented within the National Strategic Reference Framework (NSRF) 2014–2020 and co-financed by National and Community Funds (E.U.—European Social Fund).

Notes

The authors declare no competing financial interest.

REFERENCES

(1) https://apps.fas.usda.gov/psdonline/circulars/citrus.pdf (accessed May 23, 2018).

(2) Balu, A. M.; Budarin, V.; Shuttleworth, P. S.; Pfaltzgraff, L. A.; Waldron, K.; Luque, R.; Clark, J. H. Valorisation of orange peel residues: waste to biochemicals and nanoporous materials. *ChemSusChem* **2012**, *5*, 1694−1697.

(3) Pfaltzgraff, L. A. The Study & Development of an Integrated & Additive-Free Waste Orange Peel Biorefinery. Ph.D. Thesis, University of York, 2014.

(4) Pfaltzgraff, L. A.; De bruyn, M.; Cooper, E. C.; Budarin, V.; Clark, J. H. Food waste biomass: a resource for high-value chemicals. *Green Chem.* **2013**, *15*, 307−314.

(5) Kurosumi, A.; Sasaki, C.; Yamashita, Y.; Nakamura, Y. Utilization of various fruit juices as carbon source for production of bacterial cellulose by *Acetobacter xylinum* NBRC 13693. *Carbohydr. Polym.* **2009**, *76*, 333−335.

(6) George, S.; Jayachandran, K. Analysis of rhamnolipid biosurfactants produced through submerged fermentation using orange fruit peelings as sole carbon source. *Appl. Biochem. Biotechnol.* **2009**, *158*, 694−705.

(7) Rivas, B.; Torrado, A.; Torre, P.; Converti, A.; Domínguez, J. M. Submerged citric acid fermentation on orange peel autohydrolysate. *J. Agric. Food Chem.* **2008**, *56*, 2380−2387.

(8) Oberoi, H. S.; Vadlani, P. V.; Madl, R. L.; Saida, L.; Abeykoon, J. P. Ethanol Production from Orange Peels: Two-Stage Hydrolysis and Fermentation Studies Using Optimized Parameters through Experimental Design. *J. Agric. Food Chem.* **2010**, *58*, 3422−3429.

(9) Tsouko, E.; Kourmentza, C.; Ladakis, D.; Kopsahelis, N.; Mandala, I.; Papanikolaou, S.; Koutinas, A.; et al. Bacterial Cellulose Production from Industrial Waste and by-Product Streams. *Int. J. Mol. Sci.* **2015**, *16*, 14832−14849.

(10) Kuo, C.-H.; Huang, C. Y.; Shieh, C. J.; Wang, H. M. D.; Tseng, C. Y. Hydrolysis of orange peel with cellulase and pectinase to produce bacterial cellulose using *Gluconacetobacter xylinus*. *Waste Biomass Valorization* **2017**, 1−9.

(11) Hestrin, S.; Schramm, M. Synthesis of cellulose by *Acetobacter xylinum*. 2. Preparation of freeze-dried cells capable of polymerizing glucose to cellulose. *Biochem. J.* **1954**, *58*, 345−352.

(12) Klemm, D.; Heublein, B.; Fink, H. P.; Bohn, A. Cellulose: fascinating biopolymer and sustainable raw material. *Angew. Chem., Int. Ed.* **2005**, *44*, 3358−3393.

(13) Siró, I.; Plackett, D. Microfibrillated cellulose and new nanocomposite materials: a review. *Cellulose* **2010**, *17*, 459−494.

(14) De France, K. J.; Hoare, T.; Cranston, E. D. Review of Hydrogels and Aerogels Containing Nanocellulose. *Chem. Mater.* **2017**, *29*, 4609−4631.

(15) de Melo, E. M.; Clark, J. H.; Matharu, A. S. The Hy-MASS concept: hydrothermal microwave assisted selective scissoring of cellulose for in situ production of (meso)porous nanocellulose fibrils and crystals. *Green Chem.* **2017**, *19*, 3408−3417.

(16) de Assis, C. A.; Houtman, C.; Phillips, R.; Bilek, E. M. T.; Rojas, O. J.; Pal, L.; Peresin, M. S.; Jameel, H.; Gonzalez, R. Conversion Economics of Forest Biomaterials: Risk and Financial Analysis of CNC Manufacturing. *Biofuels, Bioprod. Biorefin.* **2017**, *11*, 682−700.

(17) Shi, Z.; Zhang, Y.; Phillips, G. O.; Yang, G. Utilization of bacterial cellulose in food. *Food Hydrocolloids* **2014**, *35*, 539−545.

(18) *Polymer Data Handbook*, 2nd ed.; Mark, J. E., Ed.; Oxford University Press: Oxford, U.K., 2009.

(19) Segal, L.; Creely, J. J.; Martin, A. E., Jr.; Conrad, C. M. An Empirical Method for Estimating the Degree of Crystallinity of Native Cellulose Using the X-Ray Diffractometer. *Text. Res. J.* **1959**, *29*, 786−794.

(20) Lie, S. The EBC-Ninhydrin Method for Determination of Free Alpha Amino Nitrogen. *J. Inst. Brew.* **1973**, *79*, 37−41.

(21) Wu, J. M.; Liu, R. H. Thin stillage supplementation greatly enhances bacterial cellulose production by *Gluconacetobacter xylinus*. *Carbohydr. Polym.* **2012**, *90*, 116−121.

(22) Vazquez, A.; Foresti, M. L.; Cerrutti, P.; Galvagno, M. Bacterial cellulose from simple and low cost production media by *Gluconacetobacter xylinus*. *J. Polym. Environ.* **2013**, *21*, 545−554.

(23) Chen, L.; Hong, F.; Yang, X. X.; Han, S. F. Biotransformation of wheat straw to bacterial cellulose and its mechanism. *Bioresour. Technol.* **2013**, *135*, 464−468.

(24) Guo, X.; Cavka, A.; Jönsson, L. J.; Hong, F. Comparison of methods for detoxification of spruce hydrolysate for bacterial cellulose production. *Microb. Cell Fact.* **2013**, *12*, No. 93.

(25) Hong, F.; Guo, X.; Zhang, S.; Han, S. F.; Yang, G.; Jönsson, L. J. Bacterial cellulose production from cotton-based waste textiles: enzymatic saccharification enhanced by ionic liquid pretreatment. *Bioresour. Technol.* **2012**, *104*, 503−508.

(26) Pacheco, G.; Nogueira, C. R.; Meneguin, A. B.; Trovatti, E.; Silva, M. C.; Machado, R. T.; Barud, H. D. S.; et al. Development and characterization of bacterial cellulose produced by cashew tree residues as alternative carbon source. *Ind. Crops Prod.* **2017**, *107*, 13−19.

(27) Moon, S. H.; Park, J. M.; Chun, H. Y.; Kim, S. J. Comparisons of physical properties of bacterial celluloses produced in different culture

DOI: 10.1021/acsomega.8b01315
ACS Omega 2018, 3, 10365−10373

conditions using saccharified food wastes. *Biotechnol. Bioprocess Eng.* **2006**, *11*, 26−31.
(28) Castro, C.; Zuluaga, R.; Putaux, J. L.; Caro, G.; Mondragon, I.; Ganán, P. Structural characterization of bacterial cellulose produced by *Gluconacetobacter swingsii* sp. from Colombian agroindustrial wastes. *Carbohydr. Polym.* **2011**, *84*, 96−102.
(29) Adebayo-Tayo, B. C.; Akintunde, M. O.; Sanusi, J. F. Effect of different fruit juice media on bacterial cellulose production by *Acinetobacter* sp. BAN1 and *Acetobacter pasteurianus* PW1. *J. Adv. Biol. Biotechnol.* **2017**, *14*, 1−9.
(30) Sabiha-Hanim, S.; Aziatul-Akma, A. Polymer Characterization of Cellulose and Hemicellulose. In *Polymer Science: Research Advances, Practical Applications and Educational Aspects*; Méndez-Vilas, A.; Solano-Martín, A., Eds.; Formatex Research Center: Spain, 2016.
(31) Kim, Y.-M.; Lee, H. W.; Kim, S.; Watanabe, C.; Park, Y.-K. Non-Isothermal Pyrolysis of Citrus Unshiu Peel. *BioEnergy Res.* **2015**, *8*, 431−439.
(32) Wada, M.; Okano, T.; Sugiyama, J. Synchrotron-radiated X-ray and neutron diffraction study of native cellulose. *Cellulose* **1997**, *4*, 221−232.
(33) Sugiyama, J.; Persson, J.; Chanzy, H. Combined infrared and electron diffraction study of the polymorphism of native celluloses. *Macromolecules* **1991**, *24*, 2461−2466.
(34) Lee, C. M.; Gu, J.; Kafle, K.; Catchmark, J.; Kim, S. H. Cellulose produced by *Gluconacetobacter xylinus* strains ATCC 53524 and ATCC 23768: Pellicle formation, post-synthesis aggregation and fiber density. *Carbohydr. Polym.* **2015**, *133*, 270−276.
(35) Watanabe, K.; Tabuchi, M.; Morinaga, Y.; Yoshinaga, F. Structural Features and Properties of Bacterial Cellulose Produced in Agitated Culture. *Cellulose* **1998**, *5*, 187−200.
(36) Park, S.; Baker, J. O.; Himmel, M. E.; Parilla, P. A.; Johnson, D. K. Cellulose crystallinity index: measurement techniques and their impact on interpreting cellulase performance. *Biotechnol. Biofuels* **2010**, *3*, No. 10.
(37) Liitiä, T.; Maunu, S. L.; Hortling, B.; Tamminen, T.; Pekkala, O.; Varhimo, A. Cellulose crystallinity and ordering of hemicelluloses in pine and birch pulps as revealed by solid-state NMR spectroscopic methods. *Cellulose* **2003**, *10*, 307−316.
(38) Bernardinelli, O. D.; Lima, M. A.; Rezende, C. A.; Polikarpov, I.; Ribeiro deAzevedo, E. Quantitative ^{13}C MultiCP solid-state NMR as a tool for evaluation of cellulose crystallinity index measured directly inside sugarcane biomass. *Biotechnol. Biofuels* **2015**, *8*, No. 110.
(39) Tuinier, R.; ten Grotenhuis, E.; Holt, C.; Timmins, P. A.; de Kruif, C. G. Depletion interaction of casein micelles and an exocellular polysaccharide. *Phys. Rev. E* **1999**, *60*, No. 848.
(40) Wachirasiri, P.; Julakarangka, S.; Wanlapa, S. The effects of banana peel preparations on the properties of banana peel dietary fibre concentrate. *Songklanakarin J. Sci. Technol.* **2009**, *31*, 605.

DOI: 10.1021/acsomega.8b01315
ACS Omega 2018, 3, 10365−10373